# Silicon/Silicon Carbide/Graphite Composite Anode Material for Rechargeable Lithium-Ion Batteries by High-Temperature Vacuum Adsorption Method

[1]Liyong Wang, [1]Mei Wang, [1]Huiqi Wang[*], [2]Jinhua Yang[**], [1]Shengsheng Ji, [1]Lei Liu
[1]Shengliang Hu and [3]Quangui Guo[***]

[1]*School of Energy and Power Engineering, North University of China, Taiyuan 030001, PR China.*
[2]*National Key Laboratory of Advanced Composites, AECC Beijing Institute of Aeronautical Materials, Beijing 10095, PR China.*
[3]*CAS Key Laboratory of Carbon Materials, Institute of Coal Chemistry, Chinese Academy of Sciences, Taiyuan 03l0001, PR China.*
hqiwang@nuc.edu.cn; yangjinhua08@163.com; qgguo@sxicc.ac.cn; nucc@nuc.edu.cn

(Received on 13th July 2023, accepted in revised form 19th March 2024)

**Summary:** Recently, the electrode materials for next-generation lithium-ion batteries (LIBs) draw widespread attention on storing reversibly the electrical energy. For this issue, the expanded graphite and silicon particles are chosen to generate silicon/silicon carbide/graphite composite anode material using a high-temperature vacuum adsorption method. The prepared composites are measured by X-ray diffraction, transmission electron microscopy, and Raman spectra, et al. The composites are cycled at a current density of 50 mA $g^{-1}$, in order to observe their potential specific capacity. An initial charge capacity is 566.5 mAh $g^{-1}$, and its initial Coulombic efficiency is 97.4 %. The reversible specific capacity keeps at 502 mAh $g^{-1}$ after 80 cycles, displaying a capacity retention of 88.7%.

**Keywords:** Silicon, Expanded graphite, Lithium-ion battery, Anode, High-temperature vacuum adsorption.

## Introduction

To decrease the $CO_2$ emission and environmental pollution, the green energy is of concern of all over the world now. As the demand for enormous energy, the lithium-ion batteries (LIBs) have aroused wide public concern, because they can store reversibly electrical energy [1]. LIBs have been commercially fabricated in the world for many years. They are applied in electric vehicles, mobile phones, and various power stations in the global market [2, 3]. However, the energy storage properties of LIBs will to be improved a bit further to meet the higher demand of electric devices. They are studied and described through energy density, power density, life time, capacity, electrochemical properties and physical electrode properties [4-11]. Many issues are related to the integrated multidisciplinary knowledge. The traditional current collector of LIBs is metal, which has good electric conductivity. Recently, carbon based current collectors are being researched, which include graphene film, flexible graphite film, and carbon nanotube papers. They can not only provide good electric conductivity, but also provide outstanding corrosion resistance, and good thermal conductivity [12-14]. Anode materials mainly include carbon materials, semiconductor alloy, and metal oxide [6, 8, 10, 15-19]. Graphite has three-dimensional structure, which contains graphite layers and Van der Waals force bonds between graphite layers. The graphite anode material has a lower capacity than that of the Si, and is 372 mAh $g^{-1}$ [8, 20-24]. The traditional commercial graphite anode materials can usually obtain a capacity near to 370 mAh $g^{-1}$, which is limited by the lithium storage mechanism of the ideal graphite.

Si has emerged as a potential anode material for LIBs. However, it undergoes volumetric expansion (~400 %) during the alloying-dealloying reactions with Li. Only through drastic volume change, Si can get a balance to realize the alloying with Li to get the highest specific capacity. The Si's theoretical capacity is about 4200 mAh $g^{-1}$, which has been a potential candidate as negative material for LIBs [25, 26]. Though it has the higher capacity than other materials (such as graphite, germanium, metal oxide, and so on),

[*]**To whom all correspondence should be addressed.**

it encounters volume changes during the cycling process, which results in the degradation of electrochemical performance, such as devastating volume expansion, labile solid electrolyte interphase (SEI) and poor electric conductivity [27-31]. Because of these issues, Si based anode materials cannot take place of commercial graphite anodes in the market. One approach was to utilize nanostructured Si, which could deal with such challenges to utilize the drastic volume expansion to get good electrochemical performance. It could relieve the pulverization because the smaller size could relax the stress during the drastic volume expansion to enhance cycle lives. Additionally, such nanostructured Si also could shorten the Li diffusion distance and enhance the electroactivity. The examples include Si nanowire, Si nanotubes, Si nanoparticles and porous structured composites, which could have a stable SEI.

Facing the requirement of the high performance of anode material for LIBs, the silicon carbide (SiC) has also been studied [32]. SiC layers were investigated by the first principles calculations as anode material for LIBs. Its activation energy was 0.046 eV, and the diffusion coefficient was at the order 10-11 $m^2/s$ [33]. This also indicated SiC to be a new potential anode material for LIBs. Using PECVD method, the nanocrystalline SiC film was fabricated as anode material. The SiC film's thickness was 150 nm. It got a specific capacity of 309 mAh $g^{-1}$ after 60 discharge-charge process [34]. Inspired by the experimental research, many methods and strategies were tried to improve the electrochemical property of the SiC anode. Porous structure design was used in preparing the anode materials [35-40]. Porous structure could enhance the mechanical strength, and increase materials' specific surface area, which improved the electrochemical properties of anode materials.

The porous structured SiC was prepared, and showed a power and energy performance of 400 W/Kg and 350 Wh/Kg during the first cycle (125 mA $g^{-1}$), respectively. The porous structured SiC obtained good electron conductivity and $Li^+$ ion diffusivity. The electrolyte resistance and charge transfer resistance of SiC electrode was measured to be 24.5 and 250 Ω. And it had a $Li^+$ ion diffusion coefficient of $6.54 \times 10^{-19}$ $cm^2\ s^{-1}$. Judging from the above results, the SiC will have a potential application on LIBs [41]. The batteries were tested at current density of 1.25A/g, the corresponding specific power and energy were more than 3000 W/kg and 130 Wh/kg after 130 cycles, which were higher than that of the prepared Si anode.

Biomass derived materials usually could be used to store energy, which was low cost and obtained from a wide range of sources. The SiC derived from agricultural waste was prepared for LIBs. The SiC/hard carbon composites obtained a capacity of 950 mAh $g^{-1}$ after 600 cycles. The prepared composite electrode almost had almost no volume expansion on charge-discharge process, comparing with that of Si anode [42]. The Si and carbon (C) can be acquired from the environment-benign biological materials. Cycled at 1 A $g^{-1}$, the C-SiC composite derived from the rice husks got a capacity of over 1000 mAh $g^{-1}$ after long cycles [43].

In view of the above work, SiC could be prepared by different raw materials using chemical methods. Inspired by the experimental work, using the high-temperature vacuum adsorption method, expanded graphite and commercial silicon particles were chose to fabricate SiC. The expanded graphite was prepared using traditional method [44]. The prepared Si/SiC/graphite composite material for rechargeable LIBs was studied in the work. During the first cycle, an initial discharge and charge capacities of 581.9 and 566.5 mAh $g^{-1}$ were obtained, with a Coulombic efficiency of 97.4%. Measured at a current density of 50 mA $g^{-1}$, its reversible capacity kept at 502 mAh $g^{-1}$ after 80 cycles. It also got a good rate capability, which could restore to the initial capacity (564.5 mAh $g^{-1}$). A high-temperature vacuum adsorption method to prepare Si/SiC/graphite composite anode material was demonstrated in this work.

## Experimental

### *Raw materials and methods*

The expanded graphite was prepared by traditional method in the laboratory. The Si nanoparticles were purchased in the market (Xuzhou Jiechuang Material Technology Co., LTD). The method for preparing composite was shown in Fig.1. The expanded graphite was first compressed by a mold, which had a plan view size of 2 $cm^2$ and thickness of 0.5 cm. Then it was covered by Si powder with a mass ration of 1:1.2 in a ceramic ark. The Si has a higher density than that of the expanded graphite, hence, the mass ratio was tried to be set at 1:1.2. The composite materials were treated at 1773 K under vacuum atmosphere in the tube furnace.

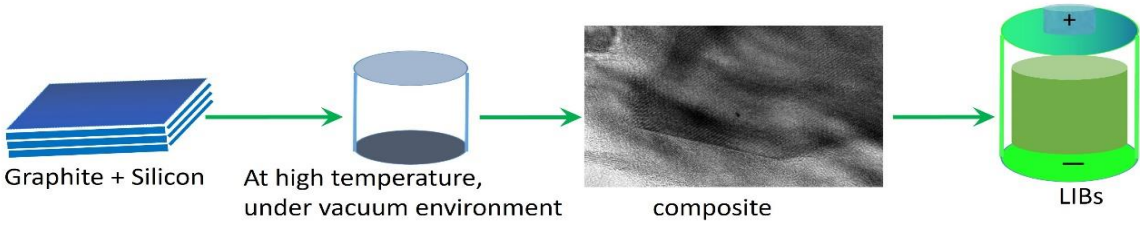


Fig. 1: Schematic illustration of the fabrication process of the Si/SiC/graphite composites.

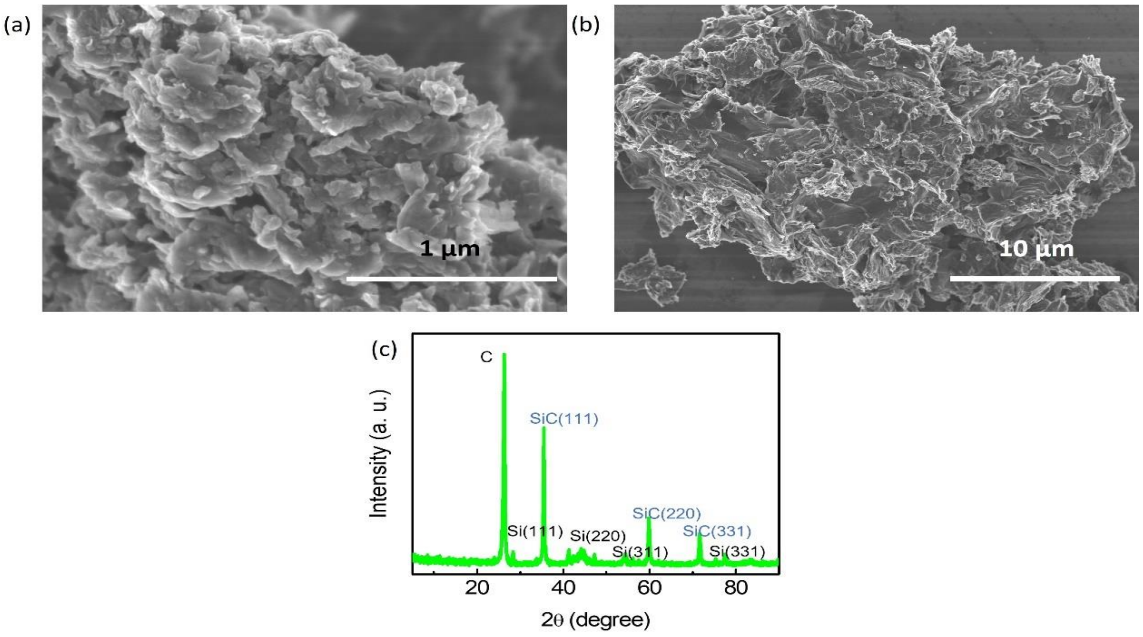


Fig. 2: SEM images of the Si/SiC/graphite composites (a, b), and the XRD pattern of the composites (c).

*Characterizations and Electrochemical Evaluation*

The crystallite structure of materials was examined by X-ray diffraction system (XRD; Bruker AXS D8, Karlsruhe, German). The morphology of the prepared samples was looked into by Field-emission scanning electron microscopy (SEM, JSM-7001F, JEOL, Tokyo, Japan). The microstructure of the samples was observed by field-emission transmission electron microscopy (TEM, JEM-2100F, JEOL, Tokyo, Japan). The molecular structure information of the samples was studied by the Raman spectra (HORIBA Jobin Yvon, LabRam HR800, λ=532 nm, Paris, France). Information about solid surfaces of samples was observed by X-ray photoelectron spectroscopy (XPS; Al Ka source,15 KV, 20 mA).

The coin cells were prepared as half cells in a glovebox with Ar atmosphere. The counter electrode and reference electrode were the lithium foil. The average weight of the active material of anode material was 5.97 mg. The separator was purchased in the market (Celgard 2400, South Lakes Drive, Charlotte, NC, USA). The commercial electrolyte was applied in the experiment. 1 M $LiPF_6$ was mixed with ethylene carbonate-dimethyl carbonate (1:1 by volume) and 5 vol. % vinylene carbonate. The battery test system was used to observe the electrochemical property of the samples (LAND CT 2001A model, Wuhan Jinnuo Electronics Ltd., Wuhan, China). The voltage range was 0.01-3V at room temperature. The electrochemical impedance diagram was measured by

electrochemical workstation (CHI660E, Shanghai, China).

**Results and Discussion**

The expanded graphite and silicon powder generated SiC at high temperature under vacuum environment. The Fig. 2(a, b) depicted the morphology of the prepared Si/SiC/graphite composites. The surface appearance of the composites looked like blocks stacking together in the Fig. 2b. The XRD spectrum was added in Fig. 2c. The C peak (2θ=26.3°) represented carbon structure, which was derived from the expanded graphite. And the weak Si peaks represented the Si powder. The SiC's three (111), (220), and (311) typical crystal orientations were denoted to three crystal peaks located at 2θ=35.5°, 59.82°, and71.58°.[41, 45]

The mapping analysis was chosen to observe the element distribution in the prepared Si/SiC/graphite composites in Fig. 3(a, b). The Si signal could be observed between the micro blocks. The red dots were on behalf of the Si element in Fig. 3c. The green dots represented the C element in Fig. 3d. The element of the composite was consistent with the experimental design.

The microstructure of the Si/SiC/graphite composites was shown in Fig.4a. The obvious bright spots indicated its good crystal structure in the mapping pattern. The graphite-derived lattice bands of carbon were displayed in bottom left of the Fig.4b. The SiC crystal structure was marked on the figure. Both the SiC and graphite's crystal structure demonstrated a high level of crystallization. The electrical conductivity of the composite anode might benefit from this.

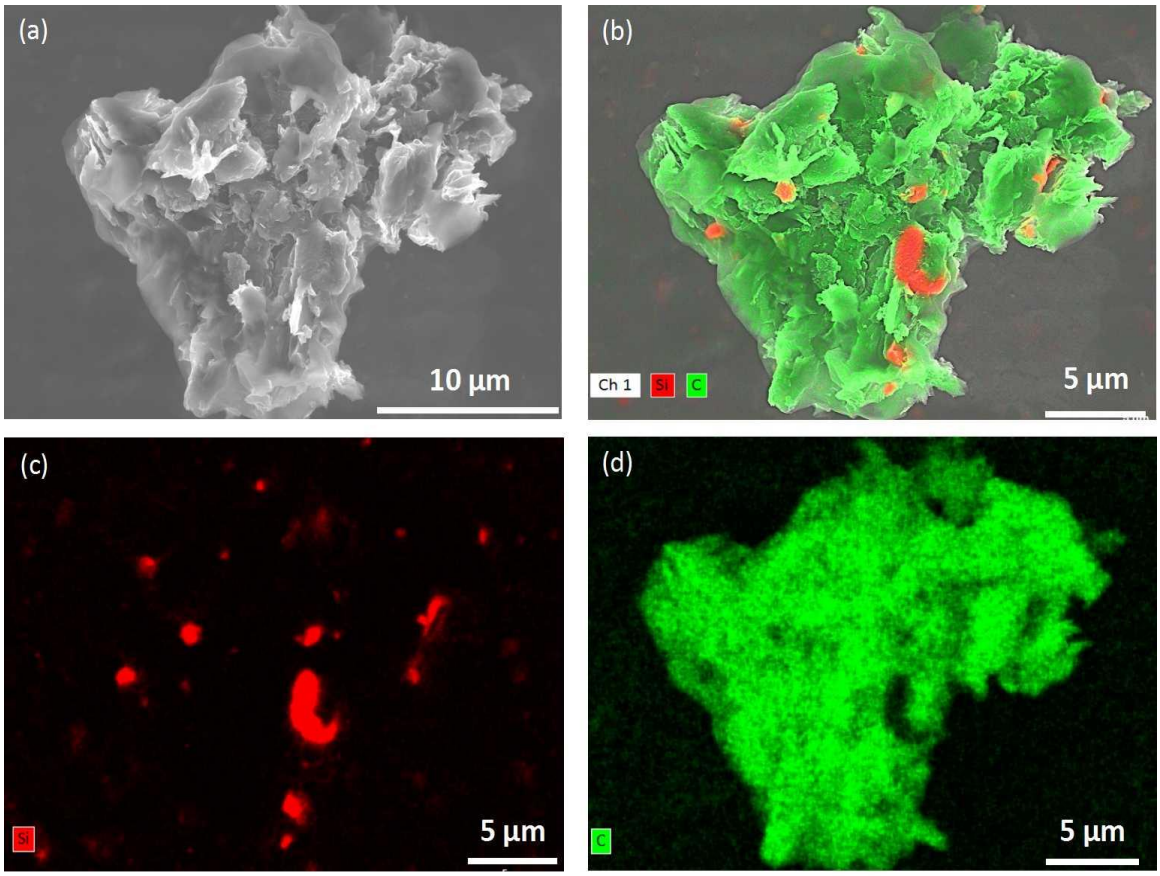


Fig. 3: SEM imagines and mapping analysis of prepared Si/SiC/graphite composites (a, b). The Si element distribution map (c), the carbon element distribution map (d).

The crystallite of the prepared composites was determined using Raman spectroscopy. As shown in Fig. 5a, carbon materials had two main bands in the Raman spectra [46, 47]. The defect lattice vibration mode (D band) was located at 1349.85 $cm^{-1}$, which was related to the defect structure of the carbon material. The 1578.64 $cm^{-1}$ peak represented the graphitic lattice vibration mode (G band). The shoulder peak (D′peak) was at 1618.73 $cm^{-1}$. The T+D peak was found at 2449.94 $cm^{-1}$ in the spectra. The SiC's Raman peaks were located at 788 and 959 $cm^{-1}$, respectively, as shown in Fig. 5 (b, c) [48-50].

Fig. 6 displayed the XPS survey of the prepared Si/SiC/graphite composites. The photoemission peaks of silicon (Si2s and Si2p), carbon (C1s), and oxygen (O1s) were showed in the spectrum. The C1s peak was located at 284.83 eV, which was related to the graphite substrate in the prepared samples in the Fig. 6a [51]. The O1s peak was tested at 532.08 eV, which might be caused by mild oxidation after long-time exposure to the air. The Si2p peak was demonstrated at 100.73eV attributing to Si-C. And the Si2s's peak was at 152.08 eV [52, 53]. In view of the above results, the composite mainly contained Si and C element.

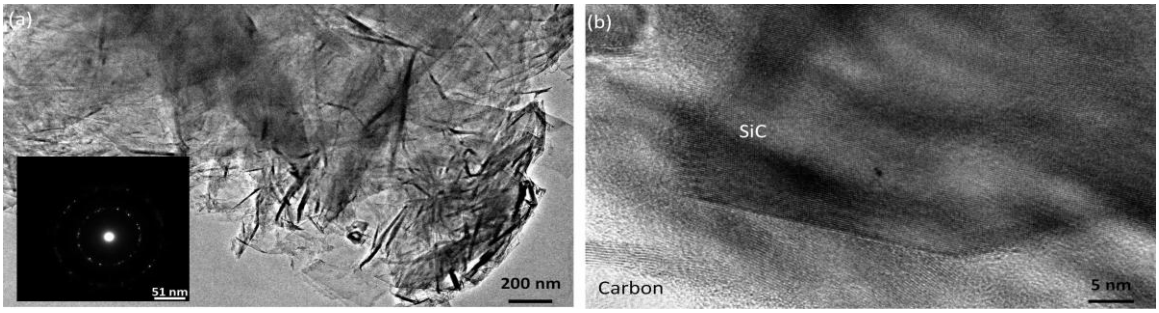


Fig. 4: TEM images and mapping analysis of the Si/SiC/graphite composites (a, b).

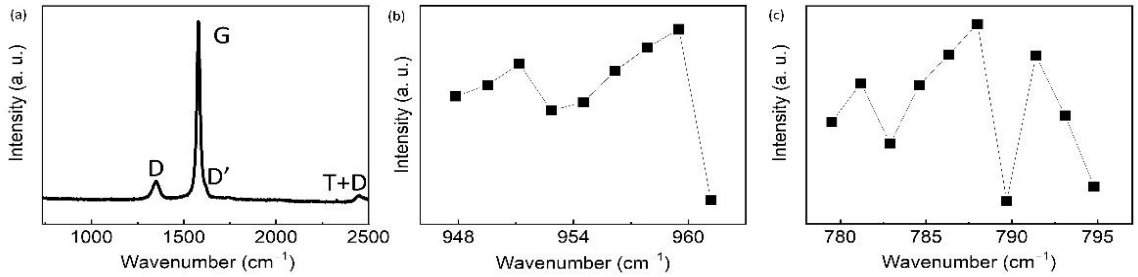


Fig. 5: Raman spectra of the Si/SiC/graphite composites: graphite peaks (a), SiC peaks (b, c).

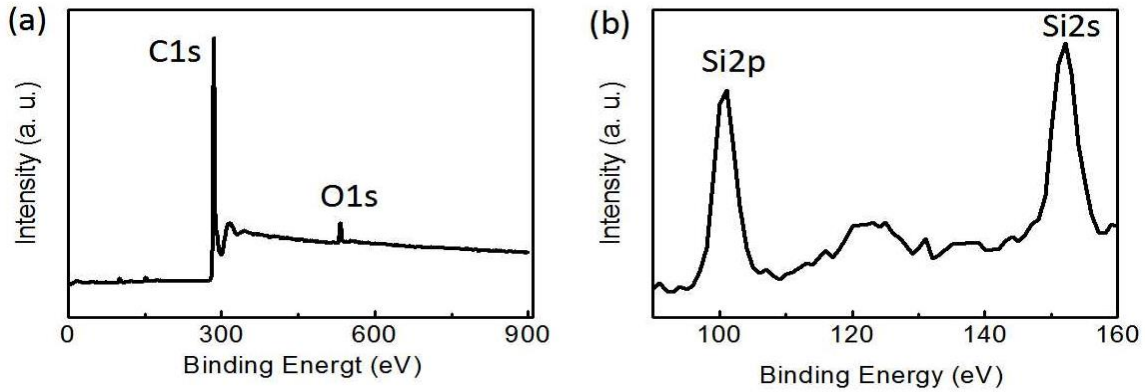


Fig. 6: XPS survey of Si/SiC/graphite composites: (a) the C1s and O1s peaks, (b) the Si2s and Si2p peaks.

Fig. 7a depicted the electrochemical property of the Si/SiC/graphite composites. The cells were first cycled at a low current density of 50 mA $g^{-1}$, the composites' first charge capacity was 566.5 mAh $g^{-1}$, corresponding to a Coulombic efficiency of 97.4 %. After 80 cycles, the final capacity kept at 502 mAh $g^{-1}$. During the whole process, the average capacity was 576 mAh $g^{-1}$. The capacity was attributed to the joint contribution of the Si nanoparticles, SiC, and expanded graphite.

Rate capability was used to investigate the cycle capability at different current densities as shown in Fig. 7b. The composites delivered the capacity of 527.4, 461, and 371 mAh $g^{-1}$ after fifth, tenth, and fifteenth cycle. The reversible capacity decreased due to the growing current density. When cycled at a current density of 1 A $g^{-1}$, it had a capacity of 212.3 mAh $g^{-1}$. After the high-rate measurements, the current density was switched back to of 50 mA $g^{-1}$. It recovered to a capacity of 564.5 mAh $g^{-1}$ near to that of the first five cycles. The voltage platform located at about 0.24 V, in which the composites got half the reversible charging capacity. The 1$^{st}$, 40$^{th}$, and 80$^{th}$ cycle curves were shown in Fig. 7c. It did not have huge specific capacity attenuation compared with that of pure Si nanoparticles. The electrochemical performance of pure Si nanoparticles was described in Fig. 7d. The first charge capacity was 2994 mAh $g^{-1}$. But after 6 cycles the specific capacity reduced to less than 1000 mAh $g^{-1}$.

Fig. 7 depicted a typical cyclic voltammetry (CV) measurement of the Si/SiC/graphite composites. The voltage range was 0.01-3.0 V. The sweep rate was set at 1 mV/s. An obvious anodic peak at 0.192 V was seen in the anodic scan, and the cathodic peak was at 0.173 V in the Fig. 7. The corresponding peaks and curves overlapped well during the subsequent scan, which indicated good electrochemical performance.

The composites were examined by electrochemical impedance spectroscopy (EIS) measurements. Fig. 7 had two semicircles and a straight short slopping line [54, 55]. The formation of the SEI might be related to the first semicircle at the high frequency region. There was a semicircle in the medium frequency region, which was probably related to the interfacial charge transfer impedance. The lithium diffusion impedance was mostly responsible for the straight, short-slopping line at low frequency. The composites might have enhanced the diffusion and transport of lithium ions between the electrode and the electrolyte, according to the straight diffusion tail.

The electrolyte resistance was represented by Re in the equivalent circuit shown in Fig. 7h, while $R_{ct}$ denoted the charge transfer resistance (145 Ω) and $R_f$ represented the resistance of the surface film and contact (110 Ω). Additionally, $Z_w$ indicated the Warburg impedance of the composite electrode.

In the previous research, graphite has a theoretical capacity of 372 mAh $g^{-1}$ [56], and silicon nanowires can obtain a capacity of 3150 mAh $g^{-1}$ [25]. Compared with that of graphite and silicon, pure silicon carbide's specific capacity can maintain at 309 mAh $g^{-1}$, which has no design on structure [34]. Silicon carbide/hard carbon composite can keep a capacity of 950 mAh $g^{-1}$ after 600 cycles, which is higher than that of the SiC anode. The silicon/graphite microspheres/carbon composites (P-Si/C) have high capacity of 474 mAh $g^{-1}$ after 100 cycles. In the composites, graphite microspheres and amorphous carbon can be used as buffers in lithium-silicon alloys during charge process. Amorphous carbon effectively connects silicon with the GMs, forming a highly conductive network for composites.

The coatings structural design can give rise to the steady performance for LIBs. The designed p-SiOx/SiC@C anode can reach more than 700 mAh $g^{-1}$ at 0.1 A $g^{-1}$, and its capacity remains unchanged after 100 cycles [57]. The SiC/C composite are prepared to be mesoporous nanotubes as anode material, which has kept 527 mAh $g^{-1}$ after 250 cycles. Although the novel structural design can bring about the improvement of electrochemical performance, it may not be conducive to the production and preparation of enterprises in the market. Herein, this work proposes a high-temperature vacuum adsorption method to fabricate Si/SiC/graphite composite anode material for LIBs by one-step procedure in the work. It can supply a steady capacity of 502 mAh $g^{-1}$ after 80 cycles. This method does not contain complicated process compared with previous research work.

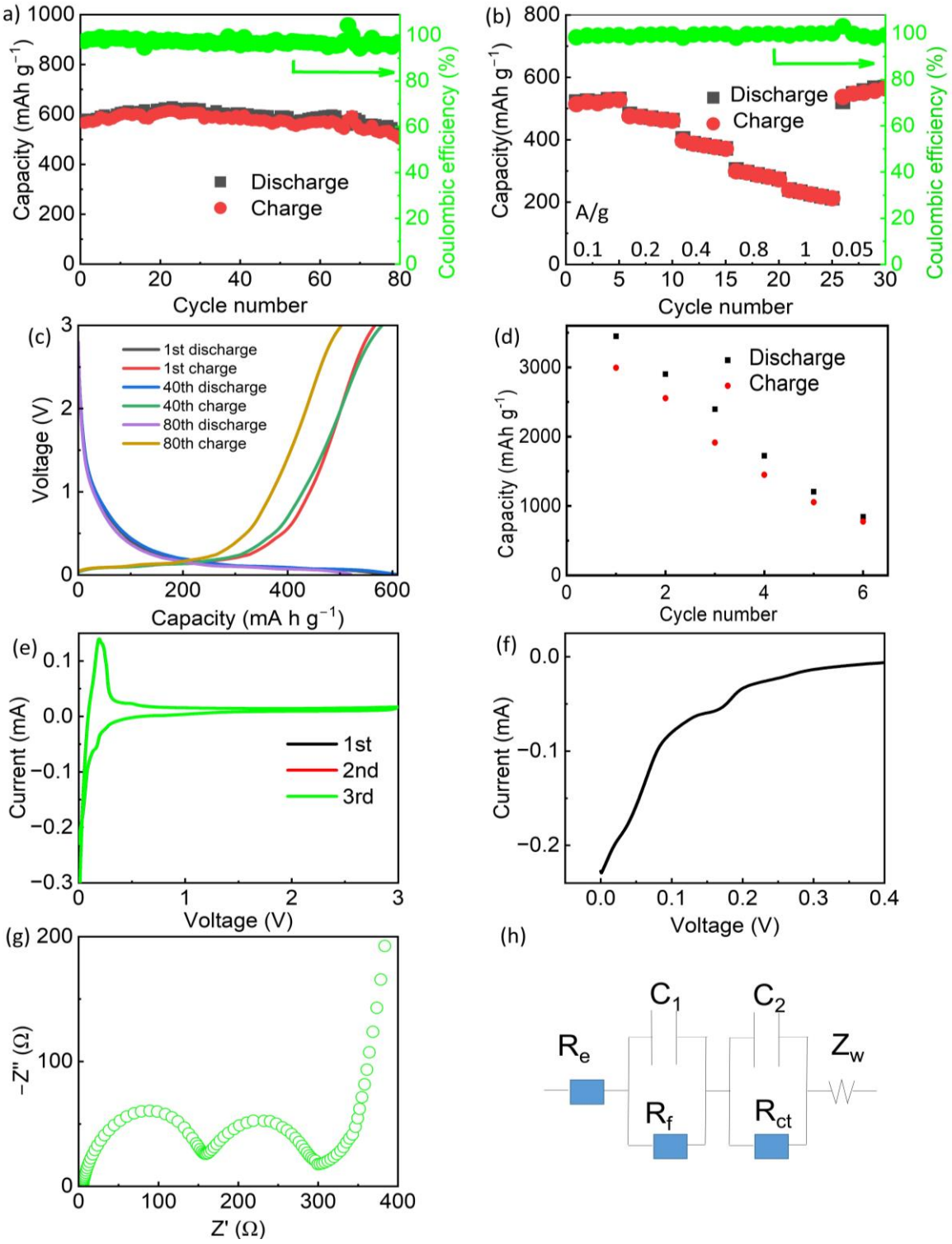


Fig. 7: Electrochemical properties of the Si/SiC/graphite composites: (a) Cycle performance, (b) Rate capability, (c) Discharge-charge curves, (e, f) Cyclic voltammetry curves, (g) Nyquist plots. (h) The equivalent circuit of the composites. (d) Cycle performance of the pure Si nanoparticles.

Table-1: Summary of findings of silicon carbide composite materials for LIBs anode.

| Number | Sample | Current | Cycle number | Capacity (mAh $g^{-1}$) | Reference |
|---|---|---|---|---|---|
| 1 | Graphite | | | 372 | [56] |
| 2 | Silicon nanowires | C/20 | 10 | 3150 | [25] |
| 3 | SiC | C/10 | 60 | 309 | [34] |
| 4 | SiC/hard carbon | C/10 | 600 | 950 | [42] |
| 5 | P-Si/C | 50 mA/g | 100 | 474 | [58] |
| 6 | P-$SiO_2$/SiC@C | 100 mA/g | 100 | 837 | [57] |
| 7 | SiC/C | 100 mA/g | 250 | 527 | [59] |
| 8 | Si/SiC/graphite | 50 mA/g | 80 | 502 | This work |

After cycling, the cells were disassembled to observe the morphology of the Si/SiC/graphite composites using the SEM and TEM. As illustrated in Fig. 8 (a, b, c), a homogeneous blending of the composites was observed. Energy dispersive X-ray spectroscopy (EDS) analysis was performed on the designated region shown in Fig. 8c, revealing predominantly carbon and silicon elements with a minor presence of oxygen element, which aligned with the intended design specifications. No additional elements were detected within the composites.

The microstructure of the Si/SiC/graphite composites was analyzed using TEM, and the results are presented in Fig.9. In Fig.9a, a complex intertwining between the graphite structure and SiC crystal structure can be observed. Additionally, electron diffraction pattern obtained from the entire area of Fig.9a revealed a slight degree of disorder (as shown in Fig.9c). The graphite's crystal structure could be observed obviously in Fig.9b.

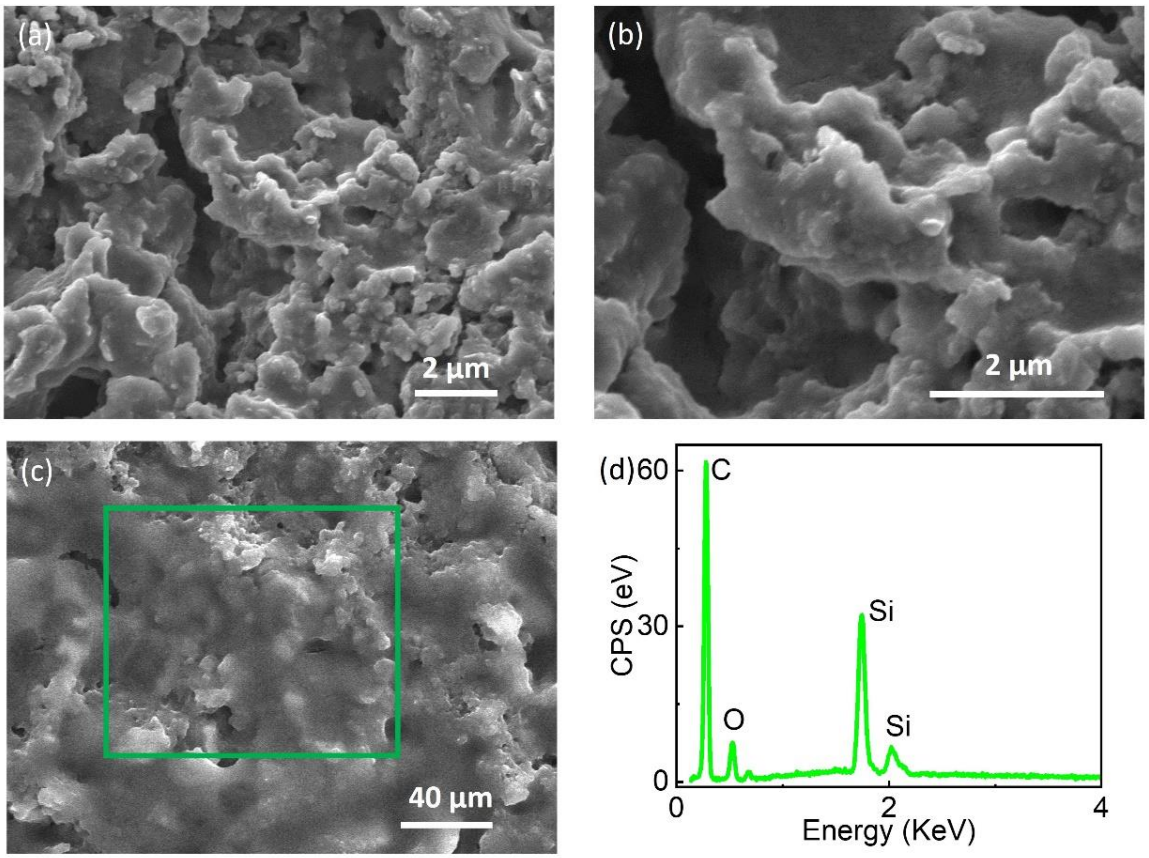


Fig. 8: SEM imagines of the Si/SiC/graphite composites after cycling (a, b, c). (d) EDS of the marked area of (c).

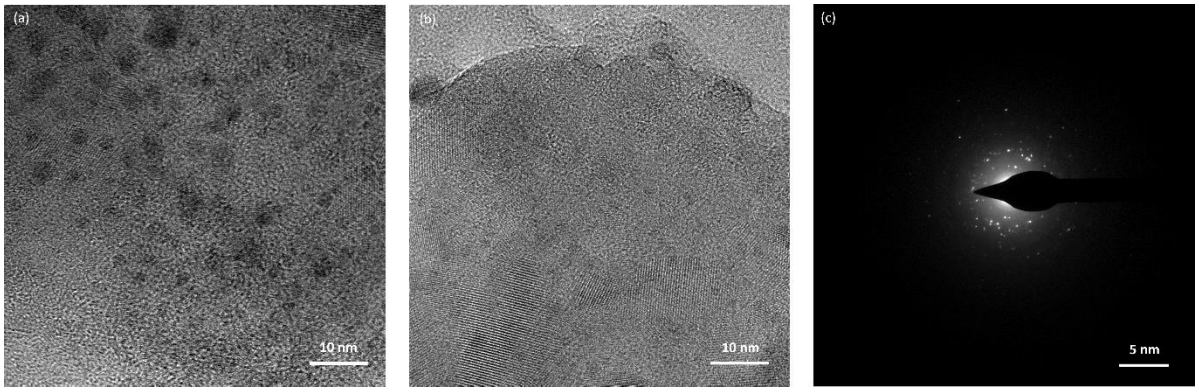


Fig. 9: TEM images of the Si/SiC/graphite composites after cycling (a, b). (c) The electron diffraction pattern taken from the entire area of (a).

## Conclusions

In conclusion, the expanded graphite and silicon particles were used to generate Si/SiC/graphite composites. Both the SiC and graphite's crystal structure help to improve the anode's electrical conductivity because of their high level of crystallization. Tested at a low current density of 50 $mAg^{-1}$, the prepared cell got the first discharge and charge capacity of 581.9 and 566.5 mAh $g^{-1}$, respectively. The initial Coulombic efficiency was 97.4 %. After 80 cycles, its capacity kept at 502 mAh $g^{-1}$, displaying capacity retention of 88.7%. It displayed a good rate capability, which could restore to the initial capacity (564.5 mAh $g^{-1}$). A high-temperature vacuum adsorption method to fabricate Si/SiC/graphite composite anode material for LIBs was demonstrated by one-step procedure in the work.

## Acknowledgements

This work was supported by the Fundamental Research Program of Shanxi Province (No. 202303021211161, No. 20210302123052, 201901D211270), the Key Research and Development (R&D) Projects of Shanxi Province (No. 202102040201003), and the Graduate Student Education Innovation Projects of Shanxi Province (No. 2020SY352, 2020SY355), National Natural Science Foundation of China (No. 62205311).

## References

1. L. A. Román-Ramírez, J. Marco, Design of experiments applied to lithium-ion batteries: A literature review, *Applied Energy*, **320,** 119305 (2022).
2. L. Lander, E. Kallitsis, A. Hales, J.S. Edge, A. Korre, G. Offer, Cost and carbon footprint reduction of electric vehicle lithium-ion batteries through efficient thermal management, *Applied Energy*, **289,** 116737 (2021).
3. L. Yang, Y. Cai, Y. Yang, Z. Deng, Supervisory long-term prediction of state of available power for lithium-ion batteries in electric vehicles, *Applied Energy*, **257,** 114006 (2020).
4. F. Duffner, N. Kronemeyer, J. Tübke, J. Leker, M. Winter, R. Schmuch, Post-lithium-ion battery cell production and its compatibility with lithium-ion cell production infrastructure, *Nature Energy*, **6,** 123 (2021).
5. P. Li, H. Kim, K. H. Kim, J. Kim, H. G. Jung, Y. K. Sun, State-of-the-art anodes of potassium-ion batteries: synthesis, chemistry, and applications, *Chemical Science*, **12,** 7623 (2021).
6. C. Meng, M. Yuan, B. Cao, X. Lin, J. Zhang, A. Li, X. Chen, M. Jia, H. Song, Laser-modified graphitic onion-like carbon as anode for lithium/potassium-ion batteries, *Carbon*, **192,** 347 (2022).
7. S. Fugattini, U. Gulzar, A. Andreoli, L. Carbone, M. Boschetti, P. Bernardoni, M. Gjestila, G. Mangherini, R. Camattari, T. Li, S. Monaco, M. Ricci, S. Liang, D. Giubertoni, G. Pepponi, P. Bellutti, M. Ferroni, L. Ortolani, V. Morandi, D. Vincenzi, R.P. Zaccaria, Binder-free nanostructured germanium anode for high resilience lithium-ion battery, *Electrochimica Acta*, **411,** 139832 (2022).
8. L. Wang, Z. Liu, Q. Guo, G. Wang, J. Yang, P. Li,

X. Wang, L. Liu, Electrochemical properties of carbon nanocoils and hollow graphite fibers as anodes for rechargeable lithium ion batteries, *Electrochimica Acta*, **199,** 204 (2016).

9. H. Wang, N. Bai, M. Wang, L. Wang, Y. Li, J. Chen, S. Hu, C. Chen, Richly electron-deficient $BC_xO_{3-x}$ anodes with enhanced reaction kinetics for sodium/potassium-ion batteries, *Materials Chemistry Frontiers*, **6,** 1882 (2022).
10. H. Q. Wang, Y. X. Zhao, L. Gou, L. Y. Wang, M. Wang, Y. Li, S. L. Hu, Rational construction of densely packed Si/MXene composite microspheres enables favorable sodium storage, *Rare Metals*, **41,** 1626 (2022).
11. L. Gou, W. Jing, Y. Li, M. Wang, S. Hu, H. Wang, Y. B. He, Lattice-Coupled Si/MXene Confined by Hard Carbon for Fast Sodium-Ion Conduction, *ACS Applied Energy Materials*, **4,** 7268 (2021).
12. Y. Ye, L. Y. Chou, Y. Liu, H. Wang, H.K. Lee, W. Huang, J. Wan, K. Liu, G. Zhou, Y. Yang, A. Yang, X. Xiao, X. Gao, D.T. Boyle, H. Chen, W. Zhang, S.C. Kim, Y. Cui, Ultralight and fire-extinguishing current collectors for high-energy and high-safety lithium-ion batteries, *Nature Energy*, **5,** 786 (2020).
13. Q. Wu, J. Yang, Y. Zhao, R. Song, Z. Wang, Z. Huang, M. Shi, Y. Ye, D. He, S. Mu, Lifting the energy density of lithium ion batteries using graphite film current collectors, *Journal of Power Sources*, **455,** 227991 (2020).
14. Y. Yang, W. Yuan, X. Zhang, Y. Ke, Z. Qiu, J. Luo, Y. Tang, C. Wang, Y. Yuan, Y. Huang, A review on structuralized current collectors for high-performance lithium-ion battery anodes, *Applied Energy*, **276,** 115464 (2020).
15. H. Wang, D. An, P. Tian, W. Jing, M. Wang, Y. Li, H. R. Li, S. Hu, T. N. Ye, Incorporating quantum-sized boron dots into 3D cross-linked rGO skeleton to enable the activity of boron anode for favorable lithium storage, *Chemical Engineering Journal*, **425,** 130659 (2021).
16. C.-L. Ma, Z.-H. Hu, N.-J. Song, Y. Zhao, Y. Z. Liu, H. Q. Wang, Constructing mild expanded graphite microspheres by pressurized oxidation combined microwave treatment for enhanced lithium storage, *Rare Metals*, **40,** 837 (2021).
17. N. Liu, K. Huo, M.T. McDowell, J. Zhao, Y. Cui, Rice husks as a sustainable source of nanostructured silicon for high performance Li-ion battery anodes, *Scientific reports*, **3,** 1919 (2013).
18. L. Zhou, J. Zhang, Y. Wu, W. Wang, H. Ming, Q. Sun, L. Wang, J. Ming, H.N. Alshareef, Understanding Ostwald Ripening and Surface Charging Effects in Solvothermally-Prepared Metal Oxide–Carbon Anodes for High Performance Rechargeable Batteries, *Advanced Energy Materials*, **9,** 1902194 (2019).
19. R. Fang, K. Chen, L. Yin, Z. Sun, F. Li, H. M. Cheng, The Regulating Role of Carbon Nanotubes and Graphene in Lithium-Ion and Lithium–Sulfur Batteries, *Advanced materials*, **31,** 1800863 (2019).
20. S. Ghosh, U. Bhattacharjee, S. Patchaiyappan, J. Nanda, N.J. Dudney, S.K. Martha, Multifunctional Utilization of Pitch-Coated Carbon Fibers in Lithium-Based Rechargeable Batteries, *Advanced Energy Materials*, **11, 2**100135 (2021).
21. X. Jiang, Y. Chen, X. Meng, W. Cao, C. Liu, Q. Huang, N. Naik, V. Murugadoss, M. Huang, Z. Guo, The impact of electrode with carbon materials on safety performance of lithium-ion batteries: A review, *Carbon*, **191,** 448 (2022).
22. C. Kim, K.S. Yang, M. Kojima, K. Yoshida, Y.J. Kim, Y.A. Kim, M. Endo, Fabrication of Electrospinning-Derived Carbon Nanofiber Webs for the Anode Material of Lithium-Ion Secondary Batteries, *Advanced Functional Materials*, **16,** 2393 (2006).
23. J. H. Lin, C. Y. Chen, Thickness-controllable coating on graphite surface as anode materials using glucose-based suspending solutions for lithium-ion battery, *Surface and Coatings Technology*, **436,** 128270 (2022).
24. H. Xiao, G. Ji, L. Ye, Y. Li, J. Zhang, L. Ming, B. Zhang, X. Ou, Efficient regeneration and reutilization of degraded graphite as advanced anode for lithium-ion batteries, *Journal of Alloys and Compounds*, **888,** 161593 (2021).
25. C.K. Chan, H. Peng, G. Liu, K. McIlwrath, X.F. Zhang, R.A. Huggins, Y. Cui, High-performance lithium battery anodes using silicon nanowires, *Nature nanotechnology*, **3,** 31 (2008).
26. Q. Wang, M. Zhu, G. Chen, N. Dudko, Y. Li, H. Liu, L. Shi, G. Wu, D. Zhang, High-Performance Microsized Si Anodes for Lithium-Ion Batteries: Insights into the Polymer Configuration Conversion Mechanism, *Advanced materials*, **34,** 2109658 (2022).
27. X. Wan, T. Mu, B. Shen, Q. Meng, G. Lu, S. Lou, P. Zuo, Y. Ma, C. Du, G. Yin, Stable silicon anodes realized by multifunctional dynamic cross-linking structure with self-healing chemistry and enhanced ionic conductivity for lithium-ion batteries, *Nano Energy*, **99,** 107334 **(2022)**.
28. H. Su, X. Li, C. Liu, Y. Shang, H. Liu, Scalable

synthesis of micrometer-sized porous silicon/carbon composites for high-stability lithium-ion battery anodes, *Chemical Engineering Journal*, **451,** 138394 (2023).
29. L. Sun, Y. Liu, R. Shao, J. Wu, R. Jiang, Z. Jin, Recent progress and future perspective on practical silicon anode-based lithium ion batteries, *Energy Storage Materials*, **46,** 482 (2022).
30. H. Liu, W. Yang, S. Che, Y. Li, C. Xu, X. Wang, G. Ma, G. Huang, Y. Li, Silicon doped graphene as high cycle performance anode for lithium-ion batteries, *Carbon*, **196,** 633 (2022).
31. F. Zhao, M. Zhao, Y. Dong, L. Ma, Y. Zhang, S. Niu, L. Wei, Facile preparation of micron-sized silicon-graphite - carbon composite as anode material for high-performance lithium-ion batteries, *Powder Technology*, **404,** 117455 (2022).
32. B.J. Jeon, J.K. Lee, Electrochemical characteristics of nc-Si/SiC composite for anode electrode of lithium ion batteries, *Journal of Alloys and Compounds*, **590,** 254 (2014).
33. A. Fatima, A. Majid, S. Haider, M.S. Akhtar, M. Alkhedher, First principles study of layered silicon carbide as anode in lithium ion battery, *International Journal of Quantum Chemistry*, **122,** e26895 (2022).
**34.** H. Zhang, H. Xu, Nanocrystalline silicon carbide thin film electrodes for lithium-ion batteries, *Solid State Ionics*, **263,** 23 (2014).
35. L. Shen, Z. Wang, L. Chen, Carbon-coated hierarchically porous silicon as anode material for lithium ion batteries, *RSC Advances*, **4,** 15314 (2014).
36. D.K. Denis, F.u. Zaman, L. Hou, G. Chen, C. Yuan, Spray-drying construction of nickel/cobalt/molybdenum based nano carbides embedded in porous carbon microspheres for lithium-ion batteries as anodes, *Electrochimica Acta*, **424,** 140678 (2022).
37. H. Yang, Z. Zhang, J. Cai, B. Yang, D. Fan, F. Zhao, Preparation and electrochemical properties of porous SiO/Ni anode materials for lithium-silicon batteries, *Journal of Alloys and Compounds*, **923,** 166396 (2022).
38. H. Lin, G. Bai, Y. Zhao, Y. Zhang, H. Wang, R. Jin, Y. Huang, X. Li, Metallic 3D porous borophosphene: A high rate-capacity and ultra-stable anode material for alkali metal ion batteries, *Vacuum*, **205,** 111418 (2022).
39. Y. Zhang, Y. Zhao, G. Bai, H. Wang, R. Jin, Y. Huang, H. Lin, Y. Hu, Metallic three-dimensional porous siligraphene as a superior anode material for Li/Na/K-ion batteries, *Colloids and Surfaces A: Physicochemical and Engineering Aspects*, **652,** 129894 (2022).
40. D. Wang, H. Zhao, C. Zhang, H. Xu, J. Li, C. Han, Z. Li, S. Hua, W. Li, S. An, X. Qiu, Low-cost and high-rate porous carbon anode material for potassium-ion batteries, *Solid State Ionics*, **381,** 115944 (2022).
41. M. Nangir, A. Massoudi, Power and energy performance of porous silicon carbide anode in lithium-metal battery, *Materials Today: Proceedings*, **42,** 1534 (2021).
42. M. Yu, E. Temeche, S. Indris, W. Lai, R.M. Laine, Silicon carbide (SiC) derived from agricultural waste potentially competitive with silicon anodes, *Green Chemistry*, **24,** 4061 (2022).
43. Z. Zhao, H. Xie, J. Qu, H. Zhao, Q. Ma, P. Xing, Q. Song, D. Wang, H. Yin, Cover Feature: A Natural Transporter of Silicon and Carbon: Conversion of Rice Husks to Silicon Carbide or Carbon-Silicon Hybrid for Lithium-Ion Battery Anodes via a Molten Salt Electrolysis Approach (Batteries & Supercaps 12/2019), *Batteries & Supercaps*, **2,** 964 (2019).
44. Y. Zhong, S. Li, X. Wei, Z. Liu, Q. Guo, J. Shi, L. Liu, Heat transfer enhancement of paraffin wax using compressed expanded natural graphite for thermal energy storage, *Carbon*, **48,** 300 (2010).
45. M.J. Langenderfer, Y. Zhou, J. Watts, W.G. Fahrenholtz, C.E. Johnson, Detonation synthesis of nanoscale silicon carbide from elemental silicon, *Ceramics International*, **48,** 4456 (2022).
46. L. Wang, Z. Liu, Q. Guo, J. Yang, X. Dong, D. Li, J. Liu, J. Shi, C. Lu, L. Liu, Structure of silicon-modified mesophase pitch-based graphite fibers, *Carbon*, **94,** 335 (2015).
**47.** S. Sengupta, M. Kundu, rGO-Wrapped Hexagonal WO3 Nanorod as Advanced Electrode Material for Asymmetric Electrochemical Supercapacitors, *Energy Technology*, **11,** 2300078 (2023).
48. M. Golosov, V. Lozanov, N. Baklanova, The study of the iridium-silicon carbide reaction by Raman and IR spectroscopy, *Materials Today: Proceedings*, **25,** 352 (2020).
49. X. Wang, Y. Zhang, S. Liu, Z. Zhao, Depth profiling by Raman spectroscopy of high-energy ion irradiated silicon carbide, *Nuclear Instruments and Methods in Physics Research Section B: Beam Interactions with Materials and Atoms*, **319,** 55 (2014).
50. J. Zheng, L. Ye, M. He, D. He, Y. Huang, J. Yu, T. Chen, Electrical and optical properties of amorphous silicon carbide thin films prepared by e-beam evaporation at room temperature, *Journal*

*of Non-Crystalline Solids*, **576,** 121233 (2022).
51. Q. Liu, J. Hou, C. Xu, Z. Chen, R. Qin, H. Liu, $TiO_2$ particles wrapped onto macroporous germanium skeleton as high performance anode for lithium-ion batteries, *Chemical Engineering Journal*, **381,** 122649 (2020).
52. N.J. Sutemire, M.V. Rix, R.P. Durman, M.A. Baker, M.J. Whiting, Growth anomalies in CVD silicon carbide monofilaments for metal matrix composites, *Materialia*, **16,** 101087 (2021).
53. Z. Zhang, J. Tan, L. Cheng, W. Yang, In-situ growth of silicon carbide nanofibers on carbon fabric as robust supercapacitor electrode, *Ceramics International*, **47,** 24652 (2021).
54. X. Su, B. Sun, J. Wang, W. Zhang, S. Ma, X. He, H. Ruan, Fast capacity estimation for lithium-ion battery based on online identification of low-frequency electrochemical impedance spectroscopy and Gaussian process regression, *Applied Energy*, **322,** 119516 (2022).
55. L. Wang, M. Wang, L. Jiao, H. Wang, J. Yang, X. Dong, T. Bi, S. Ji, L. Liu, S. Hu, C. Chen, Q. Guo, Z. Liu, Pyramid-Patterned Germanium Composite Film Anode for Rechargeable Lithium-Ion Batteries Prepared Using a One-Step Physical Method, *Coatings*, **13,** 555 (2023).
56. J.R. Dahn, T. Zheng, Y. Liu, J.S. Xue, Mechanisms for Lithium Insertion in Carbonaceous Materials, *Science*, **270,** 590 (1995).
57. Y. Weng, G. Chen, F. Dou, X. Zhuang, Q. Wang, M. Lu, L. Shi, D. Zhang, In situ growth of silicon carbide interface enhances the long life and high power of the mulberry-like Si-based anode for lithium-ion batteries, *Journal of Energy Storage*, **32,** 101856 (2020).
58. K. Xiang, X. Wang, M. Chen, Y. Shen, H. Shu, X. Yang, Industrial waste silica preparation of silicon carbide composites and their applications in lithium-ion battery anode, *Journal of Alloys and Compounds*, **695,** 100 (2017).
59. C. Shao, F. Zhang, H. Sun, B. Li, Y. Li, Y. Yang, SiC/C composite mesoporous nanotubes as anode material for high-performance lithium-ion batteries, *Materials Letters*, **205,** 245 (2017).